HIGH EFFICIENCY PIEZOELECTRIC MEMS VIBRATIONAL ENERGY HARVSTERS USING (100) ORIENTED BIFEO$_3$ FILMS

M.Aramaki[1], K.Izumi[1], T.Yoshimura[1], S.Murakami[2] and N.Fujimura[1]

[1]Graduate School of Engineering, Osaka Prefecture University

[2]Technology Research Institute of Osaka Prefecture

ABSTRACT

We have developed a design principle to fabricate of high efficient piezoelectric MEMS vibrational energy harvesters (pVEHs) from the viewpoints of materials science and MEMS. Based on the principle, we propose $BiFeO_3$ films as the piezoelectric films, because it is lead free ferroelectric and has potential for high electromechanical coupling factor ($k_{31,f}^2$). To maximize the conversion efficiency of pVEHs, the microstructure and thickness of $BiFeO_3$ films were optimized. As the result, (100) oriented 1.75-µm-thick-$BiFeO_3$ films with the $e_{31,f}$ piezoelectric coefficient of -2.5 C/m^2 was obtained on Si substrate. The pVEHs using the $BiFeO_3$ films showed the mechanical quality factor of around 400 and normalized output power of 0.9 µW/mm^2/G^2.

INTRODUCTION

As the Internet of Things (IoT) has been introduced in recent years, wireless sensor networks have become important elements. Energy harvesting technology provides a promising solution to realize self-powered sensor nodes. While various environmental sources such as light, thermal gradients, motion and electromagnetic radiation are available for the harvesting, vibration energy is the most ubiquitous and accessible. In the vibration energy harvesters, several transduction methods can be used including electrostatic generation, electromagnetic induction, and piezoelectricity. Harvesters that use the piezoelectric effect have the advantages of high energy density and potential for miniaturization [1], because piezoelectric materials can convert kinetic energy into electric power directly. Therefore, piezoelectric vibrational energy harvesters (PVEHs) need to be downsized; microelectromechanical systems (MEMS) technology is useful for developing small-scale PVEHs.

Various types of piezoelectric MEMS VEHs based on the mass-spring design have been reported. $Pb(Zr,Ti)O_3$ (PZT) [2] and AlN films [3] are the most commonly used piezoelectric materials for PVEHs. PZT has high electromechanical coupling, which is important property to obtain high efficiency, but contains lead, which is toxic element. Therefore, it is difficult to utilize PVEHs using PZT for IoT. While AlN is lead free piezoelectric, it has relatively low electromechanical coupling. Thus, practical PVEHs, which can be utilized in IoT, have not been developed, yet.

The electromechanical coupling factor $k^2_{31,f}$ is the most important property for the piezoelectric films on PVEH application, because this is related to the energy conversion from the mechanical energy into electrical energy. $k^2_{31,f}$ is given by [4]

$$k_{31,f}^2 = \frac{(1-\nu)^2 e_{31,f}^2}{Y_p \varepsilon_o \varepsilon_r}, \tag{1}$$

where, ν is Poisson's ratio , Y_p is Young's modulus, $e_{31,f}$ is effective transverse piezoelectric coefficient, ε_o and ε_r are dielectric constants of vacuum and the piezoelectric film , respectively. Based on this equation, we adopt $BiFeO_3$ as piezoelectric material, because it has the relatively low dielectric constant among ferroelectric materials and remnant polarization as large as ~100 µC/cm^2 [5], which suggests that $BiFeO_3$ films have great potential to show high $k^2_{31,f}$.

In this paper, the growth condition of (100) oriented $BiFeO_3$ films to obtain high $k^2_{31,f}$ was investigated by using rf magnetron sputtering method. Then PVEHs were fabricated using the $BiFeO_3$ films and characterized the mechanical and electrical properties.

EXPERIMENT

$LaNiO_3$ films with a thickness of 140 nm were deposited on SiO_2/(100)Si substrates as bottom electrodes and buffer layer by rf magnetron sputtering system. Pressed $LaNiO_3$ powder was used as the target. The mixture of La_2O_3 and NiO powders, in which both have 99.99% purity, were calcinations at 850ºC for 2h. Sputtering was carried out at an rf power of 50 W and a total pressure of 10^{-2} Torr. The Ar/O_2 ratio and deposition temperature were 4 and 500 °C, respectively. $BiFeO_3$ films were grown on (100) $LaNiO_3/SiO_2/Si$ by using the rf magnetron sputtering system. The $BiFeO_3$ ceramic target with 20% excess Bi were used to compensate for Bi evaporation during the deposition. The substrate temperature was varied from 450 to 500 °C. The deposition pressure, Ar/O_2 ratio, and rf power were fixed at 1.0 Pa, 4, and 30 W, respectively. The thickness of the films was varied from 450 to 1750 nm. The crystalline structures of the films were investigated by X-ray diffraction (XRD) measurement. Pt top electrodes were deposited by the sputtering at room temperature. The dielectric properties were characterized using an LCR meter. The $e_{31,f}$ piezoelectric coefficients of the $BiFeO_3$ films were measured on the basis of direct piezoelectric responses. The samples were attached on Al plates. Then, strain was applied periodically to the sample by bending the Al plate using an actuator. The charge induced by the direct piezoelectric responses was measured using a lock-in amplifier. The strain was measured using a strain gauge. Using the measured charge and strain, the $e_{31,f}$ coefficient was calculated. The details of the measurement are described elsewhere [6].

For the fabrication of pVEH, silicon-on-insulator (SOI) wafers were used as substrates. The SOI substrate was oxidized, and then (100) $LaNiO_3$/Pt/Ti bottom electrodes were fabricated by the sputtering and a photolithographic process. 1750-nm-thick $BiFeO_3$ films were deposited and etching by dry process and Pt films were deposited as top

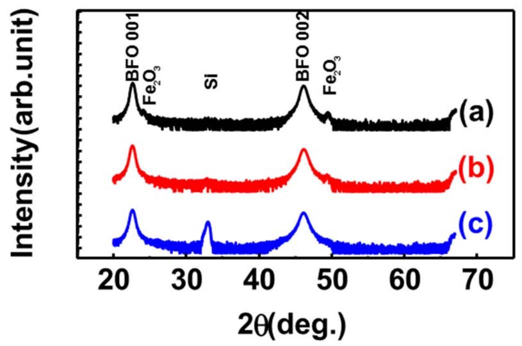

Figure 1: XRD 2θ–ω patterns of $BiFeO_3$ films deposited at (a) 500 °C, (b) 470 °C, and (c) 450 °C.

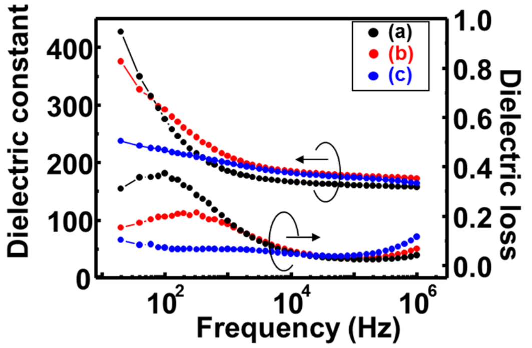

Figure 2: Frequency dependences of dielectric constant and dielectric loss of the films deposited at (a) 500 °C, (b) 470 °C, and (c) 450 °C

electrodes. Micro cantilevers with width, length, and thickness of 500, 3000, and 13 µm, respectively were fabricated by conventional MEMS process. A proof mass made of Cu was attached at the free end of the cantilever. The proof mass was approximately 1.16 mg. Vibration was applied to the pVEH in the perpendicular direction using a shaker. The applied acceleration was measured using an accelerometer. To characterize the generated electrical power of the pVEH, a load resistance was connected to the $BiFeO_3$ film. The output voltage across the load resistance was measured using a lock-in amplifier.

Results and Discussion

Figure 1 shows the XRD patterns of the films deposited from 450 to 500 °C. All the films have $BiFeO_3$ phase with (100) orientation. While the films grown at 470 °C and 500 °C have Fe_2O_3 secondary phase, the grown at 450 °C has no diffraction peak from secondary phase. It is indicated that Bi is evaporated above 470 °C during the deposition. The lattice constant of these films in c-axis is 3.93 Å, which is slightly smaller than that of the bulk (3.96 Å) [7]. It is not likely that this decrease is caused by the misfit strain by $LaNiO_3$, because the lattice constant of $LaNiO_3$ has smaller lattice constant (3.85 Å) than $BiFeO_3$, which makes a compressive strain in the $BiFeO_3$ films. Therefore, it appears that the decrease of the lattice constant is caused by the difference of the thermal expansion coefficient between $BiFeO_3$ and Si substrate. Since the thermal expansion coefficient of $BiFeO_3$ and Si is 1.9×10^{-5} K^{-1} [8] and 3.0×10^{-6} K^{-1} [9], respectively,

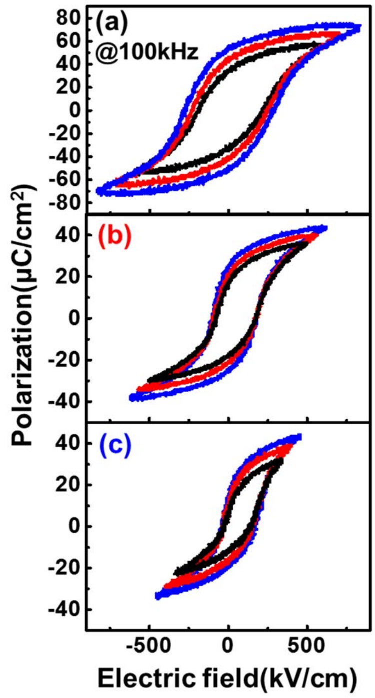

Figure 3: P-E hysteresis loops of the $BiFeO_3$ films with thicknesses of (a) 450, (b) 850, and (c) 1750 nm.

$BiFeO_3$ films receive a tensile strain from the Si substrate at room temperature. Figure 2 shows the frequency dependences of the dielectric constant and dielectric loss. The $BiFeO_3$ films deposited at 470 °C and 500 °C have the large dielectric constant and dielectric loss at low frequency. Since the dielectric loss has a peak at approximately 100 Hz, it appears that this dielectric dispersion is caused by the interface polarization due to the formation of Fe_2O_3. PVEHs are designed to have a resonant frequency of about 200 Hz to fit the frequency of ambient vibration, the large dielectric constant at low frequency decreases the electromechanical coupling factor of the $BiFeO_3$ films. Therefore, the optimum growth temperature at this deposition condition was determined as 450 °C.

$BiFeO_3$ films with thicknesses of 450, 850, and 1750nm were prepared at 450 °C. Figure 3 shows the P-E hysteresis loops of the $BiFeO_3$ films. The measurement frequency was 100 kHz. All the films show the well-defined hysteresis loops. The remnant polarization increases from 20 to 55 µC/cm^2 with decreasing the thickness. Moreover, the imprint, which is shift of the P-E loops along x axis decreases and the coercive field increase with decreasing the thickness. It is known that the imprint is caused by the internal electric field due to defects distributed along the thickness direction [10]. The coercive field decreases with decreasing the domain pinning, which is mainly caused by defects [11]. The results of P-E loops indicate that the 450-nm-thick film has high defect density with uniform distribution and with increasing the thickness, the defects has lower density and distributed along the thickness direction.

Figure 4 (a) shows the thickness dependences of $e_{31,f}$ coefficient in $BiFeO_3$ films. The films were poled at -400 kV/cm for 3 s before the measurement. The 1750-nm-thick

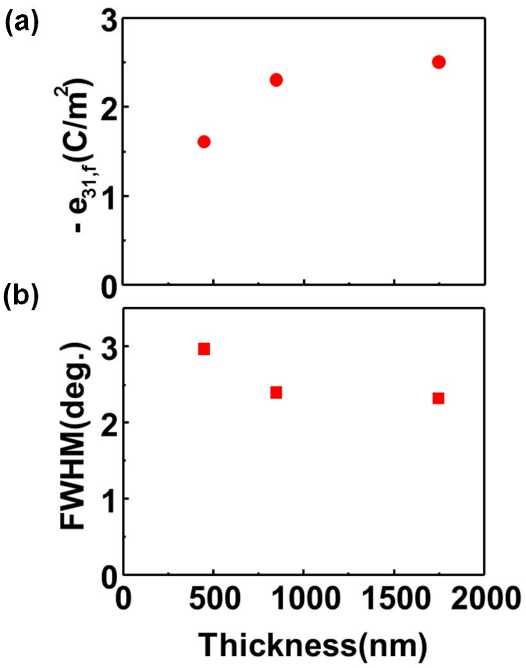

Figure 4: (a) $e_{31,f}$ as a function of film thickness. (b) FWHM as a function of film thickness of w-scan rocking curves of $BiFeO_3$(002) peak.

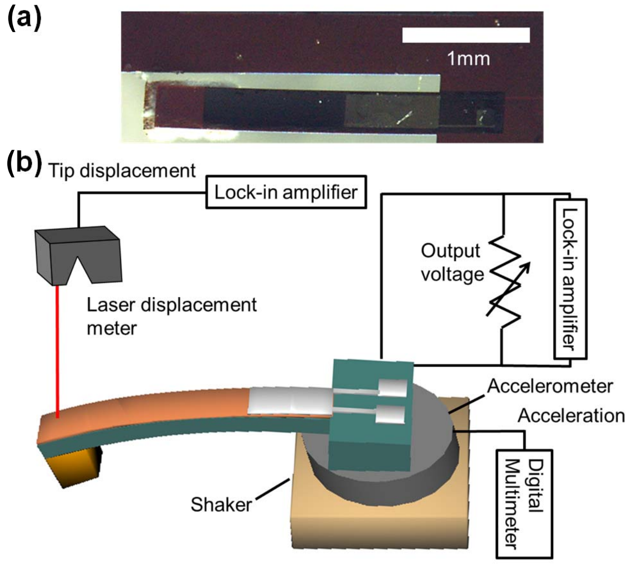

Figure 5: (a) Optical micrograph and (b) the measurement setup.

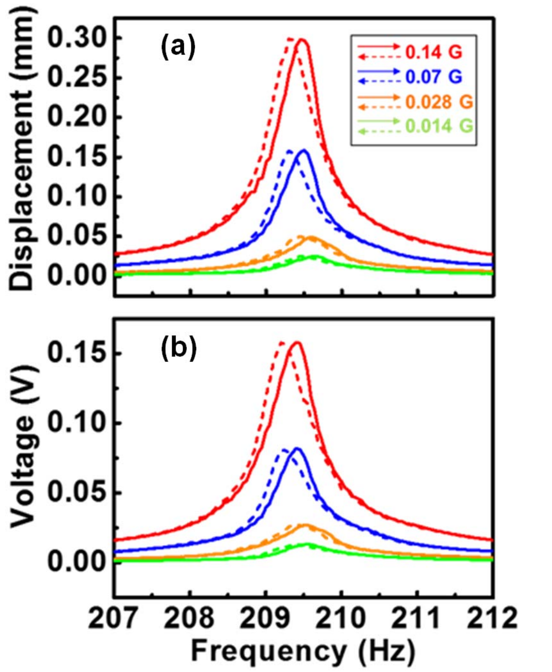

Figure 6: (a) Displacement of the mass and (b) output voltage as a function of vibrational frequency. The solid and dashed lines indicate sweep-up and sweep-down, respectively.

film shows the largest $e_{31,f}$ coefficient of -2.5 C/m^2 and $k^2_{31,}$ of 2.3%. $e_{31,f}$ coefficient suddenly decrease between the thickness of 450 nm and 850 nm. Figure 4 (b) shows the full width at half-maximum (FWHM) in rocking curves of the $BiFeO_3$ (002) peak for the 450-, 850-, and 1750-nm-thick films. FWHM decreases with increasing the thickness, which indicates the existence of the defects at the interface between bottom electrode and $BiFeO_3$ film due to the misfit. This is consistent with the results of the imprint and coercive field shown in Fig. 3 and suggests the $e_{31,f}$ coefficient of the 450-nm-thick film is lowered by the defects.

PVEHs are fabricated using the 1750-nm-thick $BiFeO_3$ film. Figure 5(a) shows the optical micrograph of the pVEHs. The micro cantilever is bended to upward direction naturally in static condition. This is consistent with the results of XRD shown in Fig. 1, which indicate that the $BiFeO_3$ film receives the tensile strain due to the difference of thermal expansion between $BiFeO_3$ and Si. Figure 5(b) shows the measurement system for pVEHs, which enable to measure the displacement of the mass and the voltage induced across the load resistance connected to the pVEHs, simultaneously. Figures 6(a) and 6(b) show the displacement of the mass measured at open circuit condition and output voltage as a function of the vibration frequency. The output voltage was measured by connecting the load resistance with 1.0 MΩ. The frequency of measurement was swept from low to high, and then reverse. The acceleration was varied from 0.014 to 0.14 G (G: gravitational acceleration). The results presented in this paper are root mean square value. The displacement and output voltage are peaked at around 209.5 Hz, which is the resonant frequency of the pVEH. The displacement and voltage increase almost linearly with increasing the acceleration. This indicates that the pVEH is in almost ideal resonance. The mechanical quality factor is one of the important parameter in pVEHs. The quality factors obtained by the ratio of the mass displacement and base displacement, FWHMs of the displacement, and voltage were 398, 418, and 380, respectively. In this experiment, the frequency was changed every 1 s. Given the quality factors of about 400, however, the period to change the frequency should be more than 3s to measure the

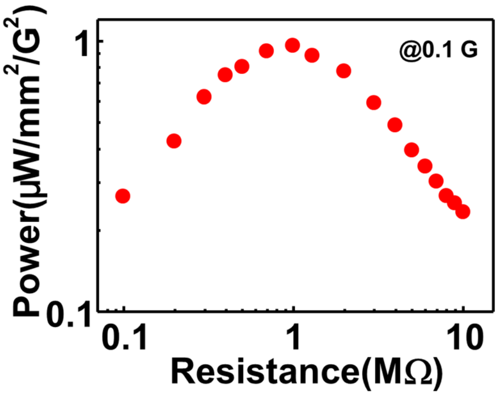

Figure 7: Normalized output power as a function of load resistance.

mechanical and electrical characteristics accurately. It seems that the small hysteresis appears in Fig. 6 mainly caused by the short period of the frequency change, which also influence the results of the quality factor. Figure 7 shows the output power as a function of load resistance. At around 1.0 MΩ, the output power shows the maximum of 0.9 $\mu W/mm^2/G^2$. This is the first demonstration of pVEHs using sputtered $BiFeO_3$ thick film.

CONCLUSIONS

To investigate the application to pVEHs, (100) oriented $BiFeO_3$ films were grown using rf magnetron sputtering system. The $BiFeO_3$ films deposited at 470 °C and 500 °C have large dielectric dispersion, which is caused by the formation of Fe_2O_3. The $BiFeO_3$ film deposited at 450ºC had no secondary phase and no dielectric dispersion. It is indicated that evaporation of Bi is suppressed at 450ºC. 450-, 850-, and 1750-nm-thick $BiFeO_3$ films deposited at 450 °C showed the well-defined P-E hysteresis loop. Form the thickness dependence of the imprint coercive field, it is suggested that the decrease of the defect density with increasing the thickness. The $e_{31,f}$ coefficient and $k^2_{31,}$of the 1750-nm-thick film is -2.5 C/m^2 and 2.3%, respectively, after poling. Cantilever-type pVEHs using the 1750-nm-thick film were fabricated using conventional MEMS process. The pVEHs had a resonant frequency of 209.5Hz, the mechanical quality factor of about 400 and normalized electric power of 0.9 $\mu W/mm^2/G^2$ at 0.1 G.

ACKNOWLEDGEMENT

This work was supported by the Industrial Technology Research Program 2011 from the New Energy and Industrial Technology Development Organization (NEDO) of Japan.

REFERENCES

[1] S. Priya, "Advances in energy harvesting using low profile piezoelectric transducers", J. ElectroCeram., vol. 19, pp. 165-182, 2007.

[2] N. Leadermann, P. Mulart, J. Baborowski, S. Gentil, K. Mukati, M. Cantoni, A. Seifert, and N. Setter, "{100}-Textured, piezoelectric $Pb(Zr_x, Ti_{1-x})O_3$ thin films for MEMS: integration, deposition and properties", Sen. Actuators A, vol. 105, pp. 162-170, 2003.

[3] M. Renaud, K. Karakaya, T. Sterken, P. Fiorini, C. Van Hoof, and R. Puers, "Fabrication, modelling and characterization of MEMS piezoelectric vibration harvesters", Sens. Actuators A, vol. 145-146, pp. 380-386, 2008.

[4] T. Yoshimura, S. Murakami, K. Wakazono, K. Kariya, and N. Fujimura, "Piezoelectric Vibrational Energy Harvester Using Lead-Free Ferroelectric $BiFeO_3$ Films" Appl. Phys. Express vol. 6, pp. 051501, 2013.

[5] J. Wu and J. Wang, J., "Orientation dependence of ferroelectric behavior of $BiFeO_3$ thin films", Appl. Phys., vol.106, pp. 10411, 2009.

[6] T.Yoshimura, H. Sakiyama, T. Oshio, A. Ashida and N. Fujimura, "Direct Piezoelectric Properties of Mn-Doped ZnO Epitaxial Films", Jpn. J. Apl.Phys., vol. 49, pp. 021501, 2010.

[7] G. Catalan and J. F. Scott, "Physics and Applications of Bismuth Ferrite", Adv. Mater., vol. 21, pp. 2463-2485, 2009.

[8] J. R. Chen, W. L. Wang, J. –B. Li, and G. H. Rao, "X-ray diffraction analysis and specific heat capacity of $(Bi_{1-x}La_x)FeO_3$ perovskites", J. Alloys Compd., vol. 459, pp. 66-70, 2008.

[9] C. H. Xu, C. Z. Wang, C. T. Chan, and K. M. Ho, "Theory of the thermal expansion of Si and diamond", Phys. Rev. B, vol. 43, pp. 5024-5027, 1991.

[10] M. Aramaki, K. Kariya, T. Yoshimura, S. Murakami, and N. Fujimura, "Thickness dependence of piezoelectric properties of $BiFeO_3$ films fabricated using rf magnetron sputtering system", Jpn. J. Appl. Phys. vol. 55, pp. 10TA16, 2016.

[11] S. Zhang, J. B. Lim, H. J. Lee, and T. R. Shrout, "Characterization of Hard Piezoelectric Lead-Free Ceramics", IEEE Trans. Ultrason. Ferroelectr. Freq. Control, vol. 56, pp. 1523-1527, 2009.

CONTACT

T. Yoshimura, tel: +81-72-254-9327; tyoshi@pe.osakafu-u.ac.jp